Longitudinal spatial coherence applied for surface profilometry

Joseph Rosen and Mitsuo Takeda

A method of optical coherence profilometry, believed to be new, is demonstrated. This method is based on the spatial, rather than the temporal, coherence phenomenon. Therefore the proposed interferometric system is illuminated by a quasi-monochromatic spatial incoherent source instead of a broadband light source. The surface profile is measured by means of shifting the spatial degree of coherence gradually along its longitudinal axis while keeping the optical path difference between the measured surface and a reference plane constant. Experimental proof of the new principle is presented. © 2000 Optical Society of America

OCIS codes: 110.4500, 120.3180, 050.1950, 100.6950, 030.1640, 120.6660.

1. Introduction

Optical coherence profilometry[1,2] and tomography[3,4] have become widely used techniques since the studies of Flournoy *et al.*[5] and later Davidson *et al.*[6] In these systems an examined sample and a reference surface are simultaneously illuminated by a broadband light source. The reflected waves from the two surfaces are interfered on the detector plane such that an event of high fringe visibility is used as a sign that the two waves from the two surfaces pass the same path length. The topography measurement is performed by means of shifting the reference mirror gradually along the propagation axis. When the detector identifies high-interference visibility, it is an indication that the corresponding part of the tested surface has the same altitude as the reference mirror. Thus, after a complete cycle of the mirror movement, one can deduce the surface profile of the sample compared with the planar reference plane.

Temporal coherence, which is the basic phenomenon behind coherence profilometry and tomography, is sometimes identified with the term longitudinal coherence.[7] This is because in many cases of interest the radiation coherence between two points along the propagation axis is determined by the radiation's temporal spectrum, as is manifested by the Wiener–Khintchine theorem.[8] However, much less attention has been given to the phenomenon of longitudinal spatial coherence.[9–12] The coherence between two points along the propagation axis can be determined purely by the extent of a quasi-monochromatic incoherent planar source according to a particular interpretation of the Van Cittert–Zerniek theorem. In this paper we move beyond this phenomenon to propose a new application for the longitudinal spatial coherence principle. We show that this effect can be useful to measure the three-dimensional profile of rough surfaces.

Unlike with spatial, with temporal coherence profilometry the tested sample should be illuminated by a broadband light source. The use of broadband sources can be a drawback in some cases. Many media in which the light propagates have an inhomogeneous spectral response. Inside the medium, either the light phase (dispersion) or amplitude (inhomogeneous absorption) might be changed. Thus such media change the statistical properties of the light and may reduce system performance. However, by use of a narrow-band source, one can fit the frequency's source to the low-absorbing spectral window of the medium. In that case, the efficiency of the propagation through the medium is relatively high, and the statistical properties of the light remain the same as in free-space propagation. Biegen demonstrated the use of a quasi-monochromatic light source in the coherence scanning interferometer microscope.[10] However, this microscope also operates on the principle of changing the path difference between the interferom-

J. Rosen (rosen@ee.bgu.ac.il) is with the Department of Electrical and Computer Engineering, Ben-Gurion University of the Negev, P.O. Box 653, Beer-Sheva 84105, Israel. M. Takeda is with the Department of Information and Communication Engineering, 1-5-1, Chofugaoka, Chofu, Tokyo, 182-8585, Japan.

Received 21 January 2000.
0003-6935/00/234107-05$15.00/0

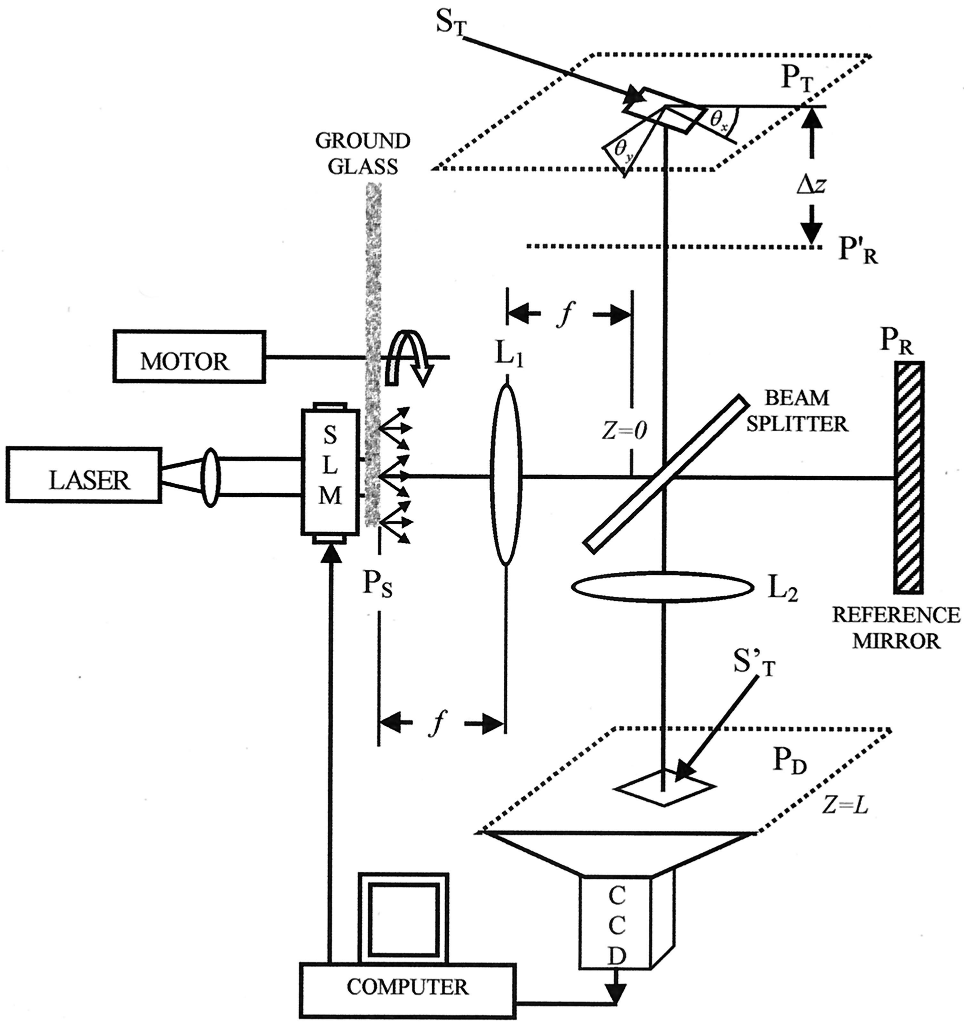

Fig. 1. Schematic of the interferometric system used for the optical spatial coherence profilometry.

eter's two arms by means of moving a reference plane. In some applications it is impossible or undesirable to change the optical path difference, for instance, when the two interferometer mirrors are rigidly connected or when the reference plane is too heavy or simply cannot be accessed for shifting.

The ability to measure surface profiles without changing the optical path difference between the interferometer's two arms is the main innovation of our system. We propose to change the shape of the light source gradually. As a result, the spatial degree of coherence progressively moves in its own space, the space (Δx, Δy, Δz) of the coordinate difference between the coherence measurement points. Thus the degree of coherence operates as a pulse of a coherence radar that detects the relative distance between the sample and the reference plane. Every time the interference visibility is high in some part of the tested surface, evidently the path difference between the constant reference mirror and this tested surface is equal to half the distance of the degree of coherence from the origin of its axis ($\Delta z = 0$). It is half the distance only because in the Michelson interferometer used here the light propagates twice along the path difference. By analyzing the events of high visibility along the degree of coherence movement, one can deduce the surface topology. Thus, unlike with other systems of this kind, we demonstrate a coherence profilometry method without changing any optical path in the interferometer. There is an additional benefit by use of longitudinal spatial, rather than temporal, coherence. The control over the complex degree of coherence by spatial masks is more flexible, and less complicated, than manipulating the source's temporal spectrum.[13,14]

2. Description of Spatial Coherence Scanning Profilometry

The scheme of our proposed system is shown in Fig. 1. A Michelson interferometer is illuminated by a quasi-monochromatic spatially incoherent light source. The source's intensity distribution is dynamically changed, owing to the combination of an electrically addressed spatial light modulator (SLM) and rotating ground glass, both illuminated by a laser. In the present experiment, because of a lack of a SLM, we instead manually changed a set of different masks to get the effect of a dynamic light source. Behind the ground glass the light passes through lens L_1 and is split into two beams. The tested surface is located at plane P_T and is used as one of the interferometer's mirrors. The other mirror at P_R is used as the reference plane. The two reflected beams from the two mirrors are combined and recorded by a CCD camera after passing lens L_2. Lens L_2 images plane P_T onto the CCD plane with the assumption that the focal depth of L_2 is long enough that all the sample points are imaged onto the CCD, although they are not necessarily located at the same distance from lens L_2.

To understand the operational principle of our method, let us consider a single reflecting plane S_T, with the smallest area that can be measured, from the entire tested surface located at plane P_T (see Fig. 1). Our goal is to measure the elevation distance Δz between plane S_T and the imaged reference plane P'_R. In addition, plane S_T is tilted relative to P'_R by angles θ_x and θ_y shown in Fig. 1. A single point from the entire source at (x_s, y_s) on the front focal plane P_S, with the amplitude $\sqrt{I_s}$, creates the following field distribution[15] behind lens L_1,

$$u(x, y, z) = \frac{[I_s(x_s, y_s)]^{1/2}}{j\lambda f} \exp\left[j\frac{2\pi(z + 2f)}{\lambda} - j\frac{2\pi}{\lambda f} \times (x_s x + y_s y) - j\frac{\pi z}{\lambda f^2}(x_s^2 + y_s^2)\right], \quad (1)$$

where λ is the light wavelength, f is the focal distance of lens L_1, and (x, y, z) are the coordinates behind lens L_1, with an origin at the back focal point. The field from every source point is split into two beams by the beam splitter. One beam is reflected from the reference mirror at P_R and interferes with the other beam reflected from the tested surface at P_T. The beam from the tested surface travels a distance $2\Delta z$ more than the other beam. As a result of the surface tilt, its reflected beam reaches the CCD plane with the angles $2\theta_x$ and $2\theta_y$ related to the z axis. For every single point source the two beams coherently interfere, because they originate from the same point source. However, since each point source is completely incoherent to any of its neighbor points, the overall intensity on the detector plane contributed from all the source points is a sum of intensities obtained from each point source. Therefore the intensity at the detector plane $z = L$ over the area of the image of S_T, denoted by S'_T, is

$$I_D(x, y, z = L)_{|(x,y)\in S'_T|} = \iint \left| \frac{[I_s(x_s, y_s)]^{1/2}}{j\lambda f} \exp\left[j\frac{2\pi(L + 2f)}{\lambda} - j\frac{2\pi}{\lambda f}(x_s x + y_s y) - j\frac{\pi L}{\lambda f^2}(x_s^2 + y_s^2)\right] + \frac{[I_s(x_s, y_s)]^{1/2}}{j\lambda f} \exp\left\{j\frac{2\pi(L + 2\Delta z + 2f)}{\lambda} - j\frac{2\pi}{\lambda f}[(x_s + \alpha_x)x + (y_s + \alpha_y)y] - j\frac{\pi(L + 2\Delta z)}{\lambda f^2}(x_s^2 + y_s^2)\right\}\right|^2 dx_s dy_s, \quad (2)$$

where $(\alpha_x, \alpha_y) = f(\sin 2\theta_x, \sin 2\theta_y)$. After straightforward algebra the intensity distribution given by Eq. (2) becomes

$$I_D(x, y, L)_{|(x,y)\in S'_T|} = A\left\{1 + |\mu(2\Delta z)|\cos\left[\frac{2\pi}{\lambda f}(\alpha_x x + \alpha_y y) - \frac{4\pi\Delta z}{\lambda} + \phi(2\Delta z)\right]\right\}, \quad (3)$$

where $A = (2/\lambda^2 f^2) \iint I_s(x_s, y_s) dx_s dy_s$. The function $\mu(\Delta z) = |\mu|\exp(j\phi)$ is the longitudinal complex degree of coherence given by

$$\mu(\Delta z) = \frac{\iint I_s(x_s, y_s)\exp\left[j\frac{\pi\Delta z}{\lambda f^2}(x_s^2 + y_s^2)\right] dx_s dy_s}{\iint I_s(x_s, y_s) dx_s dy_s}. \quad (4)$$

This final function is actually a projection on the line $(\Delta x, \Delta y, \Delta z) = (0, 0, \Delta z)$ of the three-dimensional complex degree of coherence, given by[12]

$$\mu(\Delta x, \Delta y, \Delta z) = \frac{\iint I_s(x_s, y_s)\exp\left[-j\frac{2\pi}{\lambda f}(x_s\Delta x + y_s\Delta y) + j\frac{\pi\Delta z}{\lambda f^2}(x_s^2 + y_s^2)\right] dx_s dy_s}{\iint I_s(x_s, y_s) dx_s dy_s}. \quad (5)$$

The detector records the intensity of the interference pattern between the reflected beams from the sample and from the reference mirror, as is given by Eq. (3). The visibility of these interference fringes (related to $|\mu|$) is the measured quantity. To measure the altitude of many different planes of the sample, in different altitudes, without shifting the reference mirror, two conditions should be met. The degree of the coherence function should have a delta-function-like

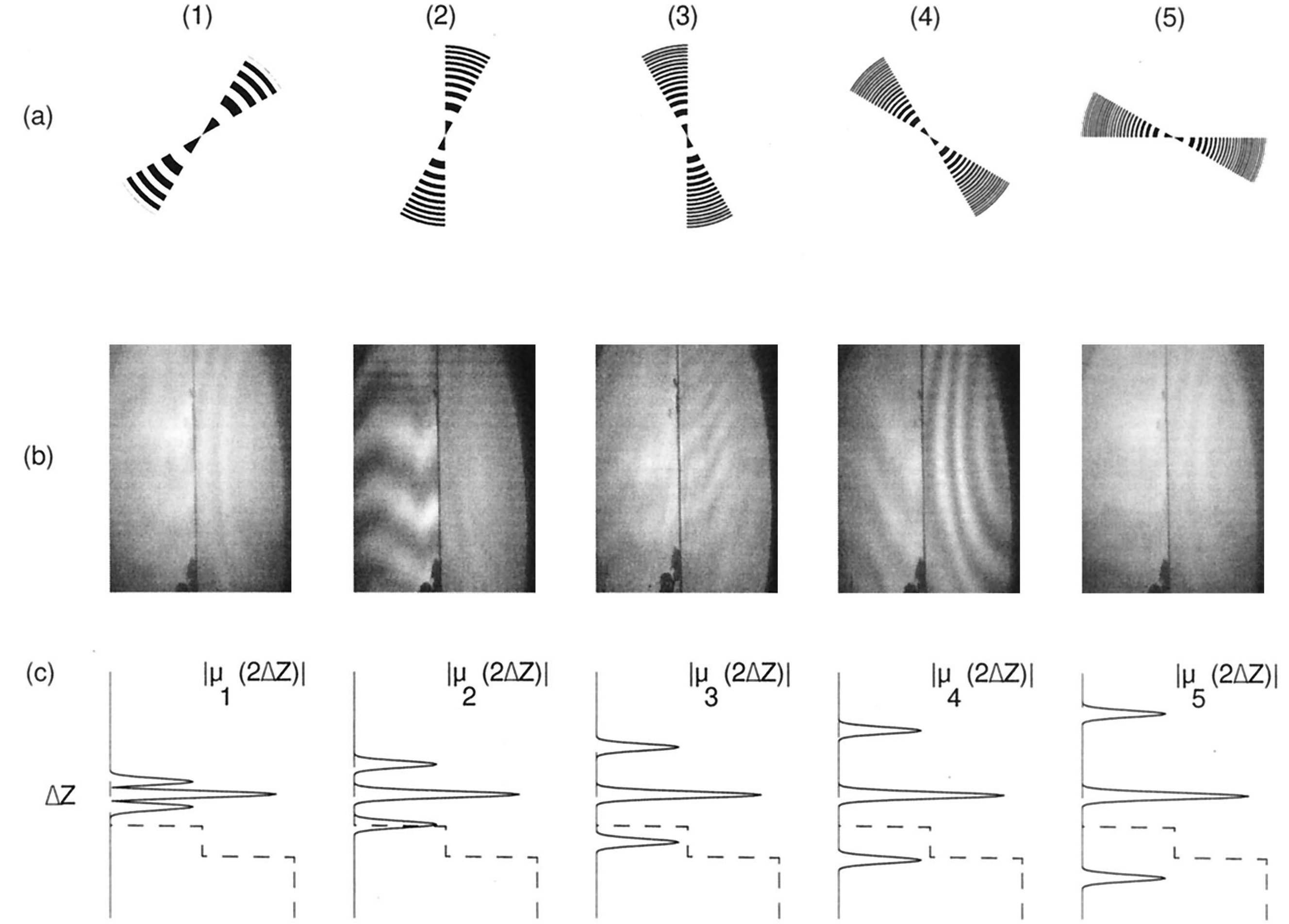

Fig. 2. (a) Set of Fresnel zone plates used to mask the light source. (b) Output images recorded by the CCD for every zone plate shown in (a). (c) Illustration of the magnitude of the complex degree of coherence for every zone plate in relation to the step of the two mirrors.

shape, and this degree of coherence should move controllably along the axis Δz. If these conditions can be achieved, each time there is a high-visibility value, the location of the degree of coherence peak is actually equal to twice the elevation Δz of the corresponding plane above (or under) the reference plane.

The degree of coherence we want to create (and then shift along Δz) originates from the spatial coherence theory. This means that it is set by the intensity distribution of a quasi-monochromatic incoherent light source according to the Van Cittert–Zernike theorem, as is explicitly manifested by Eq. (5). From analogy of Eq. (5) with the diffraction theory,[15] to create $\mu(\Delta z)$ to be as intense as possible with a peaklike shape and yet allow for its movement along the Δz axis by continually changing the shape of the source, we use the following positive real intensity distribution,

$$I_s(r_s) \propto [1 + \cos(\pi \gamma_n r_s^{\,2} + \beta_m)], \qquad 0 \le r_s \le R, \quad (6)$$

where $r_s = (x_s^{\,2} + y_s^{\,2})^{1/2}$ and R is the radius of this circular symmetric source. In this expression γ_n is a variable, which determines the location of the ± 1 Fourier orders along the Δz axis. The role of the variable β_m will be revealed below. Substituting the proposed source distribution into Eq. (4) yields the following degree of coherence,

$$\mu(\Delta z) \propto \operatorname{sinc}\left(\frac{\Delta z R^2}{2\lambda f^2}\right) * [2\delta(\Delta z) + \exp(j\beta_m)\delta(\Delta z + \gamma_n \lambda f^2) + \exp(-j\beta_m)\delta(\Delta z - \gamma_n \lambda f^2)], \qquad (7)$$

where $\operatorname{sinc}(x) = \sin(x)/x$, δ is the Dirac delta function, and $*$ denotes convolution. The desired movable peak of the degree of coherence is obtained only in the first Fourier order, and the parameter that controls its movement along the Δz axis is the grating constant γ_n. In the experimental demonstration we used a binary approximation to this cosine grating, well known as the Fresnel zone plate. By changing the zone plate constant γ_n monotonically, we scan the sample along the Δz axis. When a high-visibility peak on the curve of visibility versus γ_n is observed for some value γ_N, it is a clear indication that the location of the first-Fourier-order peak is equal to twice the distance of the tested plane from the reference plane, say, Δz_N. Thus the Nth value of γ_n reveals the altitude Δz_N according to the relation $\Delta z_N = \gamma_N \lambda f^2/2$. The depth resolution of the system is determined by the width of the first order of $\mu(\Delta z)$. According to relation (7) the smallest distinguishable altitude difference is $\Delta z_{\min} \approx 2\lambda f^2/R^2$. The transverse resolution is conventionally determined by the imaging system, represented in Fig. 1 by the combination of lens L_2 and the CCD.

In highly curved samples, where the smallest tested plane is smaller than a single fringe, the fringes can hardly be detected even under relatively high coherence. However, we can easily overcome this difficulty by using a set of values of the variable β_m suggested in relation (6). For every value of γ_n we present a few zone plates with different values of β_m distributed equally in the entire range $[0, 2\pi]$. As a result, according to relation (7), the phase of the first diffraction order of $\mu(\Delta z)$ is changed. According to Eq. (3) a change of the phase of $\mu(\Delta z)$ moves the fringes along (x, y) or along the variable m. In that case a point detector can measure the fringes' visibility, but instead of detecting the fringes in the spatial domain, they are observed along the m axis, where the m values are sampling points along a single cycle of a fringe. This technique of changing the values of β_m is extremely hard without a SLM. Therefore in the present preliminary demonstration the fringes were observed on the output plane P_D, and for all the zone plates β_m was the same.

3. Experimental Results

In the experiment a He–Ne laser with $\lambda = 0.63\ \mu$m illuminated the input mask and the rotating ground glass. The focal length L_1 was $f = 15$ cm, and the zone plates' diameter was 1 cm. As a tested surface we used a single step of two mirrors separated by a gap of 7 mm. The results of this experiment are summarized in Fig. 2. The five input masks used in the experiment are shown in Fig. 2(a). Each zone plate in this set has a different γ parameter value as follows: $\gamma_{1,\ldots,5} = 42, 74, 103, 170, 203\ \text{cm}^{-2}$. Note that each zone plate is extended over only a narrow angular zone. In this way a few zone plates could appear together on the same mask, and a rotating chopper chose a single zone plate to be illuminated for every measurement. Figure 2(b) shows the set of output interference images recorded by the CCD on plane P_D for the entire set of zone plates shown in Fig. 2(a). From these results it is clear that the high-visibility fringe pattern is obtained only on the left-hand mirror for zone plate 2 and on the right-hand mirror for zone plate 4. According to this measurement the gap between the mirrors is equal to $\Delta z_{2\text{–}4} = [(\gamma_4 - \gamma_2)\lambda f^2/2] \pm \lambda f^2/R^2 = (6.8 \pm 0.56)$ mm. Figure 2(c) illustrates the state of the function $|\mu(2\Delta z)|$ for each zone plate in relation to the altitude difference between the two mirrors shown by the dashed line. Only in the case of zone plates 2 and 4 is the distance between the zero and the first orders of μ equal to twice the distance between the reference and the two mirrors, the left- (for zone plate 2) and the right-hand (for zone plate 4) mirrors.

4. Conclusions

In conclusion, we have demonstrated the feasibility of using spatial coherence for the purpose of profilometry and tomography. A gap between two mirrors was measured by means of changing source intensity distribution and consequently shifting the spatial degree of coherence. Further progress with this technique can be achieved by use of a SLM as a tool to synthesize arbitrarily the intensity distribution of the light source. Introducing a SLM into this system will enable the detection of interference fringes in each sample point by changing the phase variable β_m in relation (6). Thus the system can be used to measure surfaces with various kinds of curves.

This study was carried out while J. Rosen was a visiting scientist at the University of Electro Communication in a binational research exchange program jointly supported by the Israel Ministry of Science and the Japan Society for the Promotion of Science. Part of this research was supported by the Israel Science Foundation.

References

1. B. S. Lee and T. C. Strand, "Profilometry with a coherence scanning microscope," Appl. Opt. **29,** 3784–3788 (1990).
2. T. Dresel, G. Hausler, and H. Venzke, "Three-dimensional sensing of rough surfaces by coherence radar," Appl. Opt. **31,** 919–925 (1992).
3. D. Huang, E. A. Swanson, C. P. Lin, J. S. Schuman, W. G. Stinson, W. Chang, M. R. Hee, T. Flotte, K. Gregory, C. A. Puliafito, and J. G. Fujimoto, "Optical coherence tomography," Science **254,** 1178–1181 (1991).
4. X. J. Wang, T. E. Milner, J. F. de Boer, Y. Zhang, D. H. Pashley, and J. S. Nelson, "Characterization of dentin and enamel by use of optical coherence tomography," Appl. Opt. **38,** 2092–2096 (1999).
5. P. A. Flournoy, R. W. McClure, and G. Wyntjes, "White-light interferometric thickness gauge," Appl. Opt. **11,** 1907–1915 (1972).
6. M. Davidson, K. Kaufman, I. Mazor, and F. Cohen, "An application of interference microscopy to integrated circuit inspection and metrology," in *Integrated Circuit Metrology, Inspection, and Process Control*, K. M. Monahan, ed., Proc. SPIE **775,** 233–247 (1987).
7. L. Mandel and E. Wolf, *Optical Coherence and Quantum Optics*, 1st ed. (Cambridge University, Cambridge, UK, 1995), Chap. 4, p. 149.
8. J. W. Goodman, *Statistical Optics*, 1st ed. (Wiley, New York, 1985), Chap. 3, p. 73 (1985); L. Mandel and E. Wolf, *Optical Coherence and Quantum Optics*, 1st ed. (Cambridge University, Cambridge, UK, 1995), Chap. 2, p. 59.
9. C. W. McCutchen, "Generalized source and the Van Cittert–Zernike theorem: a study of the spatial coherence required for interferometry," J. Opt. Soc. Am. **56,** 727–733 (1966).
10. J. E. Biegen, "Determination of the phase change on reflection from two-beam interference," Opt. Lett. **19,** 1690–1692 (1994).
11. J. Rosen and A. Yariv, "Longitudinal partial coherence of optical radiation," Opt. Commun. **117,** 8–12 (1995).
12. J. Rosen and A. Yariv, "General theorem of spatial coherence: application to three-dimensional imaging," J. Opt. Soc. Am. A **13,** 2091–2095 (1996).
13. K. Hotate and T. Okugawa, "Optical information-processing by synthesis of the coherence function," J. Lightwave Technol. **12,** 1247–1255 (1994).
14. Y. Teramura, K. Suzuki, M. Suzuki, and F. Kannari, "Low-coherence interferometry with synthesis of coherence function," Appl. Opt. **38,** 5974–5980 (1999).
15. J. Rosen and A. Yariv, "Synthesis of an arbitrary axial field profile by computer-generated holograms," Opt. Lett. **19,** 843–845 (1994).